Scattering Function and Radius of Gyration for an Interrupted Helical Chain

Yoshio Muroga

Department of Synthetic Chemistry, Faculty of Engineering, Nagoya University, Furo-cho, Chikusa-ku, Nagoya 464, Japan

Received October 8, 1991; Revised Manuscript Received February 21, 1992

ABSTRACT: The particle scattering function and also the radius of gyration are derived for an interrupted helical chain, in which helices and short-rod sequences are alternatively joined, and also for a broken helical chain, in which helices are joined with freely hinged joints. The effects of the variation in helical fraction, helical pitch, number of joints, and total number of monomer units upon the particle scattering functions are clearly observed in the normalized Kratky plot. Detailed discussion is given on the applicability of these models to the conformational analysis of amylose in aqueous solution.

Introduction

Amylose is the unbranched component of starch, and the conformations in solid state and in solution are of particular interest in macromolecular chemistry. In 1937, Hanes[1] suggested that the characteristic blue color produced on the addition of iodine to amylose solution may result from its complex with iodine in the cavity of the helical polymer chain. Rundle et al.[2,3] have shown from crystallographic studies that the amylose chain in this complex takes a helical conformation with six glucose residues per turn. Even in the absence of iodine, amylose has been found to crystallize in a number of forms, of which the most widely studied is the V-form. The conformation of amylose in the V-form has been verified as a helical chain with a pitch of 8 Å and six glucose residues per turn.[3-6]

On the other hand, the conformation of amylose in solution depends significantly on the solvents employed. In butanol and dimethylsulfoxide, it is predominantly helical, whereas in neutral aqueous solution, the overall conformation can be described as a random coil chain.[7-16] However, the local conformation of amylose in neutral aqueous solution still appears to be a matter of some controversy. Banks and Greenwood[10-13] implied that amylose in aqueous solution has no pronounced helical character. Holló and Szejtli,[17-20] Szejtli and Augustat,[21] and Senior and Hamori[22] have suggested an intact helix such as in the V-form or a broken helix, i.e., short helices joined together by hinged joints. Szejtli et al.[23,24] and Erlander et al.[25,26] suggested an interrupted helical chain, i.e., short helices joined by random coils. Pfannemüler et al.,[27] Kuge et al.,[28] and Rao et al.[29] suggested a wormlike helical chain consisting of an imperfect or a deformed helical backbone. Most of these descriptions were reviewed in the recent literature.[30,31]

Among various experimental probes to clarify the local conformation of a polymer chain in solution, the scattering function in a relatively high scattering vector region seems to be one of the most promising. The scattering function in the range of high scattering vectors can be studied by small-angle X-ray scattering or small-angle neutron scattering. Brant et al.[32] computed the theoretical scattering function, $P(h)$, for three possible models for amylose in aqueous solution, i.e., a random-coil chain model, a wormlike chain model, and an intact-helix model, on the basis of the Debye scattering equation:

$$P(h) = K^{-2}\sum_j\sum_k\left\langle\frac{\sin(hr_{jk})}{hr_{jk}}\right\rangle \qquad (1)$$

where K is the total number of scatterers, h is the magnitude of a wave vector and r_{jk} is the distance between scatterers j and k. The angle brackets express the statistical mechanical average over all conformations of a polymer chain. They accomplished the required conformational averaging of $(\sin(hr_{jk}))/hr_{jk}$ by generating various chain conformations with the Monte Carlo method under the approximation of separable chain-conformation energies. As a result, they suggested that the average conformation of amylose in aqueous solution may be represented by a tortuous random coil involving many discernible sequences of irregular short-range helical structure.[16,33,34]

Needless to say, the theoretical scattering function should be, in general, given in terms of the molecular parameters such as helical pitch, helical fraction, number of monomers per helix, and others. Although the analytical procedure of Brant et al.[32] is most instructive, it seems difficult with their procedure to incorporate these molecular parameters into the scattering function. In this paper, it is assumed that all helical and random coil portions have equal, averaged lengths respectively. If such an averaged model is allowed, the computation of the scattering function with those averaged molecular parameters can be carried out in a straightforward way. It will be shown[35] that such a model with averaged parameters is sufficiently good for computing the conformation of polypeptides, though the helical fraction and the number of monomers per helix and per random coil sequence certainly have distributions.

In the present paper, the particle scattering function and also the radius of gyration are derived in an analytical form for an interrupted helical chain, i.e., helices joined by short-rod sequences and also for a broken helical chain, i.e., helices joined by freely hinged joints, giving both helices and short-rod sequences by each averaged length. To date, these particle scattering functions have not been derived in an analytical form, although the particle scattering function for a broken rodlike chain or a freely hinged rod was given in the previous paper.[36] The present compu-

0024-9297/92/2225-3385$03.00/0

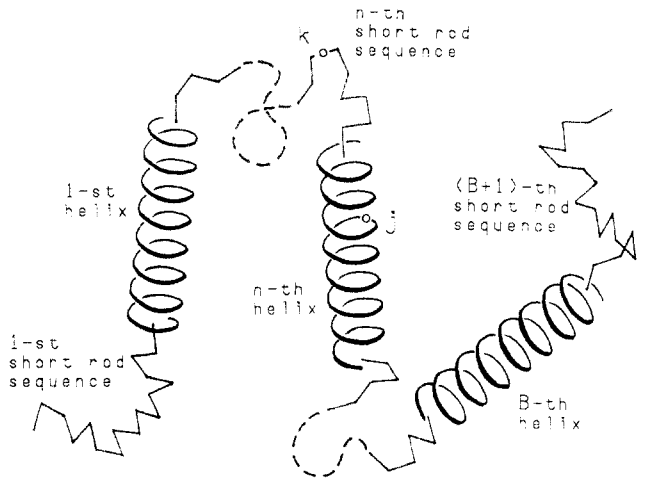

Figure 1. Interrupted helical chain represented by B helices alternatively joined by $B + 1$ short-rod sequences. Each helix has a length of p and a radius of R, and each short-rod sequence consists of M short rods of length of a.

tation is carried out by extending the procedure developed for a broken rodlike chain.[36]

Computation Result

In general, the scattering intensity is given by

$$R_\theta = \sum_j \sum_k \exp[i\vec{h}\cdot\vec{r}_{jk}] \tag{2}$$

where the wave vector $\vec{h}$ is defined

$$\vec{h} = 2\pi(\vec{s} - \vec{s}_0)/\tilde{\lambda} \tag{3}$$

$\vec{s}_0$ is the unit vector in the direction of the primary beam, $\vec{s}$ is that in the direction of the scattered beam, and $\tilde{\lambda}$ is the wavelength of the light in the solution. The absolute value of $\vec{h}$ is

$$h = (4\pi/\tilde{\lambda}) \sin(\theta/2) \tag{4}$$

where θ is a scattering angle. $\vec{r}_{jk}$ is a distance vector between the j and k scatterers.

As is shown in Figure 1, an interrupted helical chain consists of B helices joined by $B + 1$ short-rod sequences. Here, it is assumed for mathematical convenience that an end short rod in a short-rod sequence is joined with an end of the central axis of the adjacent helix, not with an end of the adjacent helical chain. Although such a model is artificial, it does not seem to give a significant effect on the final result. All short-rod sequences as well as all helices are numbered in succession: the first short-rod sequence and the first helix are numbered 1 and the last ones are numbered $B + 1$ and B, respectively. Each helix is represented by a helical curve drawn by a point rotating N times on the surface of a straight cylinder, whose height is p and radius is R, whereas each short-rod sequence consists of M short rods of length a. Free rotaion is allowed around any joint between an end of a helix and the adjacent short rod and also between adjacent short rods. The scatterers in the helix and in the short-rod sequence are respectively denoted by j and k in Figure 1, for illustration.

Using the molecular parameters thus defined, the contour length of an interrupted helical chain (L), the total number of monomers (T_n), and the helical pitch per monomer unit (P_h) are given as follows:

$$L = B\{p^2 + (2N\pi R)^2\}^{1/2} + M(B + 1)a \tag{5}$$

$$T_n = \frac{B\{p^2 + (2N\pi R)^2\}^{1/2}}{U_l} + M(B + 1) \tag{6}$$

$$P_h = \frac{pU_l}{\{p^2 + (2N\pi R)^2\}^{1/2}} \tag{7}$$

where U_l is the virtual bond length of a monomer.

Three Cartesian coordinates, x-, y-, and z-axis, in a left-handed system are fixed to each helix in a manner that the z-axis is coincident with the central axis of the helix. Three unit vectors along these axes are named $\vec{U}_x$, $\vec{U}_y$, and $\vec{U}_z$, respectively. Then, the position of a scatterer j in the mth helix, measured as a distance from the starting end of this helix, is given by following three coordinates:

$$\begin{aligned} x &= R\cos\theta_{m,j} \\ y &= R\sin\theta_{m,j} \\ z &= (p/2N\pi)\theta_{m,j} \end{aligned} \tag{8}$$

where a rotating angle $\theta_{m,j}$ is measured counterclockwise from the starting end of the helix. Moreover, a unit vector $\vec{V}_{l,h}$ ($l = 1$ to $B + 1$ and $h = 1$ to M) is fixed along the hth short rod in the lth short-rod sequence.

For computaion of the scattering intensity, eq 2, three cases are separately treated in a way similar to that in the previous paper:[35] case I is where two scatterers are in helices, case II is where they are in short-rod sequences, and case III is where one is in a helix and the other is in short-rod sequence. Thus, the total scattering intensity of eq 2, R_θ, is given as a sum of each contribution, $R_{\theta,HH}$, $R_{\theta,CC}$, and $R_{\theta,HC}$, respectively:

$$R_\theta = R_{\theta,HH} + R_{\theta,CC} + R_{\theta,HC} \tag{9}$$

Case I. If the origin 0 is placed at the beginning end of the first short-rod in the first short-rod sequence, a distance vector $\vec{r}_{m,j}$ from 0 to a scatterer j in the mth helix will be given by

$$\vec{r}_{m,j} = a\sum_{l=1}^{m}\sum_{h=1}^{M}\vec{V}_{l,h} + p\sum_{a=1}^{m-1}\vec{U}_{z,a} + \frac{p}{2N\pi}\theta_{m,j}\cdot\vec{U}_{z,m} + R\cos\theta_{m,j}\cdot\vec{U}_{x,m} + R\sin\theta_{m,j}\cdot\vec{U}_{y,m} \tag{10}$$

In a similar way, a distance vector $\vec{r}_{n,k}$ is given as follows:

$$\vec{r}_{n,k} = a\sum_{l=1}^{n}\sum_{h=1}^{M}\vec{V}_{l,h} + p\sum_{a=1}^{n-1}\vec{U}_{z,a} + \frac{p}{2N\pi}\theta_{n,k}\cdot\vec{U}_{z,n} + R\cos\theta_{n,k}\cdot\vec{U}_{x,n} + R\sin\theta_{n,k}\cdot\vec{U}_{y,n} \tag{11}$$

When expressed in the above notation, eq 2 becomes

$$R_{\theta,HH} = \sum_m\sum_n\sum_{j(m)}\sum_{k(n)}\exp[i\vec{h}\cdot(\vec{r}_{n,k} - \vec{r}_{m,j})] \tag{12}$$

When the scatterers are distributed continuously in each helix, eq 12 can be replaced by

$$R_{\theta,HH} = \sum_m\sum_n\int_0^{t_0}dt_{m,j}\int_0^{t_0}dt_{n,k}\exp[i\vec{h}\cdot(\vec{r}_{n,k} - \vec{r}_{m,j})] \tag{13}$$

where each integral is a path integral along a helical curve representing the helix and t_0 is a contour length of the curve.

Here, terms with $m = n$ are separated from those with $m \neq n$:

$$R_{\theta,\mathrm{HH}} = \sum_m S_m + \sum_n \sum_{m \neq n} S_{m,n} \tag{14}$$

where S_m is given by

$$S_m = \{(p/2N\pi)^2 + R^2\} \int_0^{2N\pi} \mathrm{d}\theta_{m,j} \int_0^{2N\pi} \mathrm{d}\theta_{m,k} \times \exp[i\vec{h}\cdot\{(p/2N\pi)\vec{U}_{z,m}(\theta_{m,k} - \theta_{m,j}) + R\vec{U}_{x,m}(\cos\theta_{m,k} - \cos\theta_{m,j}) + R\vec{U}_{y,m}(\sin\theta_{m,k} - \sin\theta_{m,j})\}] \tag{15}$$

and $S_{m,n}$ is given by

$$S_{m,n} = \{(p/2N\pi)^2 + R^2\} \int_0^{2N\pi} \mathrm{d}\theta_{m,j} \int_0^{2N\pi} \mathrm{d}\theta_{n,k} \exp[i\vec{h}\cdot\vec{v}_{m,n}] \tag{16}$$

where, if $n > m$

$$\vec{v}_{m,n} = a \sum_{l=m+1}^{n} \sum_{h=1}^{M} \vec{V}_{l,h} + p \sum_{a=m+1}^{n-1} \vec{U}_{z,a} + \frac{p}{2N\pi}\{\theta_{n,k}\vec{U}_{z,n} + (2N\pi - \theta_{m,j})\vec{U}_{z,m}\} + R(\cos\theta_{n,k}\vec{U}_{x,n} - \cos\theta_{m,j}\vec{U}_{x,m}) + R(\sin\theta_{n,k}\vec{U}_{y,n} - \sin\theta_{m,j}\vec{U}_{y,m}) \tag{17}$$

and, if $n < m$

$$\vec{v}_{m,n} = -a \sum_{l=n+1}^{m} \sum_{h=1}^{M} \vec{V}_{l,h} - p \sum_{a=n+1}^{m-1} \vec{U}_{z,a} + \frac{p}{2N\pi}\{(\theta_{n,k} - 2N\pi)\vec{U}_{z,n} - \theta_{m,j}\vec{U}_{z,m}\} + R(\cos\theta_{n,k}\vec{U}_{x,n} - \cos\theta_{m,j}\vec{U}_{x,m}) + R(\sin\theta_{n,k}\vec{U}_{y,n} - \sin\theta_{m,j}\vec{U}_{y,m}) \tag{18}$$

Since the direction of any helix and also any short rod in space is entirely independent of the directions of the others, the average of R_θ of a whole molecule over all possible conformations can be replaced by a product of each contribution from a helix and from a short rod. Denoting the averaging by $\langle\ \rangle$ and making use of the fact that the following relation holds in this case

$$\langle \exp(i\vec{\alpha}\cdot\vec{z}) \rangle = (\sin\alpha z)/\alpha z \tag{19}$$

we obtain $\langle S_m \rangle$ as follows

$$\langle S_m \rangle = \left\{\left(\frac{p}{2N\pi}\right)^2 + R^2\right\} 2 \int_0^{2N\pi} (2N\pi - z) \frac{\sin(h\sqrt{D^2})}{h\sqrt{D^2}}\,\mathrm{d}z \tag{20}$$

where

$$D^2 = \left(\frac{p}{2N\pi}\right)^2 z^2 + 4R^2 \sin^2\left(\frac{z}{2}\right) \tag{21}$$

$\langle S_{m,n} \rangle$ for $n > m$ is given by

$$\langle S_{m,n} \rangle = \left\{\left(\frac{p}{2N\pi}\right)^2 + R^2\right\} \left(\frac{\sin(hp)}{hp}\right)^{n-m-1} \times \left(\frac{\sin(ha)}{ha}\right)^{M(n-m)} \int_0^{2N\pi} \frac{\sin(h\sqrt{E^2})}{h\sqrt{E^2}}\,\mathrm{d}\theta_{n,k} \times \int_0^{2N\pi} \frac{\sin(h\sqrt{F^2})}{h\sqrt{F^2}}\,\mathrm{d}\theta_{m,j} \tag{22}$$

where

$$E^2 = \left(\frac{p}{2N\pi}\right)^2 \theta_{n,k}{}^2 + R^2 \tag{23}$$

$$F^2 = \left(\frac{p}{2N\pi}\right)^2 (2N\pi - \theta_{m,j})^2 + R^2 \tag{24}$$

$\langle S_{m,n} \rangle$ for $n < m$ is given by interchanging between m and n and between j and k in eqs 22–24. If summations in eq 14 are carried out for $\langle S_m \rangle$ and $\langle S_{m,n} \rangle$, the averaged scattering intensity, $\langle R_{\theta,\mathrm{HH}} \rangle$, is obtained as follows:

$$\langle R_{\theta,\mathrm{HH}} \rangle = 2B\left\{\left(\frac{p}{2N\pi}\right)^2 + R^2\right\}\Omega(h) + 2\left\{\left(\frac{p}{2N\pi}\right)^2 + R^2\right\}\Lambda^2(h)\left(\frac{\mu^M}{1-\mu^M\nu}\right)\left\{B - \frac{1-(\mu^M\nu)^B}{1-\mu^M\nu}\right\} \tag{25}$$

where

$$\Omega(h) = \int_0^{2N\pi} (2N\pi - z) \frac{\sin(h\sqrt{D^2})}{h\sqrt{D^2}}\,\mathrm{d}z \tag{26}$$

$$\Lambda(h) = \int_0^{2N\pi} \frac{\sin(h\sqrt{E^2})}{h\sqrt{E^2}}\,\mathrm{d}\theta_{n,k} \tag{27}$$

$$\mu = \frac{\sin(ha)}{ha} \tag{28}$$

$$\nu = \frac{\sin(hp)}{hp} \tag{29}$$

Case II. In this case, two distance vectors $\vec{r}_{m,x}$ and $\vec{r}_{n,y}$ are given as follows respectively:

$$\vec{r}_{m,x} = a \sum_{l=1}^{m-1} \sum_{h=1}^{M} \vec{V}_{l,h} + p \sum_{a=1}^{m-1} \vec{U}_{z,a} + a \sum_{i=1}^{x^0-1} \vec{V}_{m,i} + ax\vec{V}_{m,x^0} \tag{30}$$

$$\vec{r}_{n,y} = a \sum_{l=1}^{n-1} \sum_{h=1}^{M} \vec{V}_{l,h} + p \sum_{a=1}^{n-1} \vec{U}_{z,a} + a \sum_{i=1}^{y^0-1} \vec{V}_{n,i} + ay\vec{V}_{n,y^0} \tag{31}$$

where x^0 denotes the x^0th short rod in the mth short-rod sequence and x is a location in the x^0th short rod. Similar meanings are given to y^0 and y, respectively. With similar procedures as for case I, the following results are obtained:

$$\langle S_m \rangle = a^2 M\left\{2\Psi(\alpha) - \left(\frac{2}{\alpha}\right)^2 \sin^2\left(\frac{\alpha}{2}\right)\right\} + 2a^2\Psi^2(\alpha)\left(\frac{1}{1-\mu}\right)\left\{M - \frac{1-\mu^M}{1-\mu}\right\} \tag{32}$$

where

$$\alpha = ah \tag{33}$$

$$\Psi(\alpha) = \frac{1}{\alpha}\int_0^\alpha \frac{\sin t}{t}\,\mathrm{d}t \tag{34}$$

and

$$\langle S_{m,n} \rangle = 2a^2\Psi^2(\alpha)(\mu^M\nu)^{n-m}\left(\frac{1}{\mu^M}\right)\left(\frac{1-\mu^M}{1-\mu}\right)^2 \tag{35}$$

After all, the averaged scattering intensity $\langle R_{\theta,\mathrm{CC}} \rangle$ is

obtained as follows:

$$\langle R_{\theta,CC}\rangle = \sum_{n=1}^{B+1}\langle S_n\rangle + \sum_{n=1}^{B+1}\sum_{m\neq n}^{B+1}\langle S_{n,m}\rangle = a^2M(B+1)\left\{2\Psi(\alpha) - \left(\frac{2}{\alpha}\right)^2\sin^2\left(\frac{\alpha}{2}\right)\right\} + 2a^2(B+1)\Psi^2(\alpha)\left(\frac{1}{1-\mu}\right)\left\{M - \frac{1-\mu^M}{1-\mu}\right\} + 2a^2\Psi^2(\alpha)\left(\frac{1-\mu^M}{1-\mu}\right)^2 \times \left(\frac{\nu}{1-\mu^M\nu}\right)\left\{(B+1) - \frac{1-(\mu^M\nu)^{B+1}}{1-\mu^M\nu}\right\} \quad (36)$$

Case III. In this case, there are four cases for the locations of two scatterers in the chain: (a) One is in the nth helix and the other in the mth short-rod sequence and $n \geq m$. (b) One is in the nth helix and the other in the mth short-rod sequence and $n < m$. (c) One is in the nth short-rod sequence and the other in the mth helix and $n > m$. (d) One is in the nth short-rod sequence and the other in the mth helix and $n \leq m$.

For case a, two distance vectors $\vec{r}_{m,x}$ and $\vec{r}_{n,k}$ are given as follows:

$$\vec{r}_{m,x} = a\sum_{l=1}^{m-1}\sum_{h=1}^{M}\vec{V}_{l,h} + p\sum_{a=1}^{m-1}\vec{U}_{z,a} + a\sum_{i=1}^{x^0-1}\vec{V}_{m,i} + ax\vec{V}_{m,x^0} \quad (37)$$

$$\vec{r}_{n,k} = a\sum_{l=1}^{n}\sum_{h=1}^{M}\vec{V}_{l,h} + p\sum_{a=1}^{n-1}\vec{U}_{z,a} + \frac{p}{2N\pi}\theta_{n,k}\cdot\vec{U}_{z,n} + R\cos\theta_{n,k}\cdot\vec{U}_{x,n} + R\sin\theta_{n,k}\cdot\vec{U}_{y,n} \quad (38)$$

$\langle S_{m,n}\rangle$ for this case, $\langle S_{m,n}\rangle_a$, therefore, is given by

$$\langle S_{m,n}\rangle_a = a\left\{\left(\frac{p}{2N\pi}\right)^2 + r^2\right\}^{1/2}\Psi(\alpha)\Lambda(h)\left(\frac{1-\mu^M}{1-\mu}\right)(\mu^M\nu)^{n-m} \quad (39)$$

Similarly, for case b

$$\langle S_{m,n}\rangle_b = a\left\{\left(\frac{p}{2N\pi}\right)^2 + r^2\right\}^{1/2}\Psi(\alpha)\Lambda(h)\left(\frac{1-\mu^M}{1-\mu}\right)(\mu^M\nu)^{m-n-1} \quad (40)$$

It is evident that $\langle S_{m,n}\rangle_a = \langle S_{m,n}\rangle_d$ and $\langle S_{m,n}\rangle_b = \langle S_{m,n}\rangle_c$. The averaged scattering intensity, $\langle R_{\theta,HC}\rangle$, is obtained as follows:

$$\langle R_{\theta,HC}\rangle = \sum_{n=1}^{B}\sum_{m\leq n}^{B}\langle S_{m,n}\rangle_a + \sum_{n=1}^{B}\sum_{m>n}^{B+1}\langle S_{m,n}\rangle_b + \sum_{m=1}^{B}\sum_{n>m}^{B+1}\langle S_{m,n}\rangle_c + \sum_{m=1}^{B}\sum_{n\leq m}^{B}\langle S_{m,n}\rangle_d = 4a\left\{\left(\frac{p}{2N\pi}\right)^2 + R^2\right\}^{1/2}\Psi(\alpha)\Lambda(h)\left(\frac{1-\mu^M}{1-\mu}\right)\left(\frac{1}{1-\mu^M\nu}\right) \times \left\{(B+1) - \frac{1-(\mu^M\nu)^{B+1}}{1-\mu^M\nu}\right\} \quad (41)$$

The total averaged scattering intensity, $\langle R_\theta\rangle$, is given as a sum of the averaged scattering intensities for cases I–III:

$$\langle R_\theta\rangle = \langle R_{\theta,HH}\rangle + \langle R_{\theta,CC}\rangle + \langle R_{\theta,HC}\rangle \quad (42)$$

From eqs 25, 36, and 41, it can be confirmed that, when the scattering angle becomes zero, the averaged total scattering intensity, $\langle R_\theta\rangle$, tends toward the squared contour length, L^2, as it should be.

When the radius of each helix, R, becomes zero, i.e., when a polymer chain becomes B rods of length p alternatively joined together by $B+1$ short-rod sequences (called a broken rodlike chain), eqs 25, 36, and 41 are reduced as follows:

$$\langle R_{\theta,HH}\rangle/p^2 = 2B\left\{\Psi(\beta) - \left(\frac{2}{\beta^2}\right)\sin^2\left(\frac{\beta}{2}\right)\right\} + 2\Psi^2(\beta)\left(\frac{\mu^M}{1-\mu^M\nu}\right)\left\{B - \frac{1-(\mu^M\nu)^B}{1-\mu^M\nu}\right\} \quad (43)$$

where

$$\beta = ph \quad (44)$$

$$\langle R_{\theta,CC}\rangle/a^2 = M(B+1)\left\{2\Psi(\alpha) - \frac{4}{\alpha^2}\sin^2\left(\frac{\alpha}{2}\right)\right\} + 2(B+1)\Psi^2(\alpha)\left\{\frac{M}{1-\mu} - \frac{1-\mu^M}{(1-\mu)^2}\right\} + 2\Psi^2(\alpha)\left(\frac{1-\mu^M}{1-\mu}\right)^2 \times \left(\frac{\nu}{1-\mu^M\nu}\right)\left\{(B+1) - \frac{1-(\mu^M\nu)^{B+1}}{1-\mu^M\nu}\right\} \quad (45)$$

$$\langle R_{\theta,HC}\rangle/ap = 4\Psi(\alpha)\Psi(\beta)\left(\frac{1-\mu^M}{1-\mu}\right)\left(\frac{1}{1-\mu^M\nu}\right) \times \left\{(B+1) - \frac{1-(\mu^M\nu)^{B+1}}{1-\mu^M\nu}\right\} \quad (46)$$

Equations 43, 45, and 46 are coincident with those for a broken rodlike chain, which were derived in the previous paper.[36]

Furthermore, by imposing an additional condition that the length of a short rod, a, or the number of short rods in a short-rod sequence, M, becomes zero, eq 43 can be reduced to the form for B freely hinged rods of length p:

$$\langle R_\theta\rangle/p^2 = 2B\left\{\Psi(\beta) - \left(\frac{2}{\beta^2}\right)\sin^2\left(\frac{\beta}{2}\right)\right\} + 2B\Psi^2(\beta)\left(\frac{1}{1-\nu}\right) - 2\Psi^2(\beta)(1-\nu^B)\left(\frac{1}{1-\nu}\right)^2 \quad (47)$$

Equation 47 is the same one as that was originally derived by Hermans and Hermans.[37]

As is well-known, at a sufficiently small scattering angle to satisfy $\langle R_g^2\rangle h^2 < 1$, the scattering function, $P(h)$, should follow the standard expression

$$\frac{\langle R_\theta\rangle}{L^2}(\equiv P(h)) = 1 - \frac{h^2\langle R_g^2\rangle}{3} + \ldots \quad (48)$$

where $\langle R_g^2\rangle$ is a mean-squared radius of gyration. From eqs 25, 36, 41, and 48, we get the radius of gyration for an interrupted helical chain as follows:

$$\langle R_g^2\rangle = \left[f^2\left\{R^2 - \frac{R^2}{B}\left(\frac{\sin N\pi}{N\pi}\right)^2 + \frac{p^2}{12B} + \frac{(B-1)p^2}{6} + \frac{(B-1)(B+1)Ma^2}{6B}\right\} + (1-f)^2\left\{\frac{a^2}{12M(B+1)} + \frac{M(B+1)a^2}{6} - \frac{a^2}{6} + \frac{B^2p^2}{6(B+1)} + \frac{Bp^2}{3(B+1)}\right\} + 2f(1-f)\left\{\frac{R^2}{2} + \frac{Bp^2}{6} + \frac{Ma^2}{6}\left(B+\frac{1}{2}\right) - \frac{1}{12}a^2\right\}\right] \quad (49)$$

where f is a fraction of an integrated contour length of helical portions against a contour length of a whole

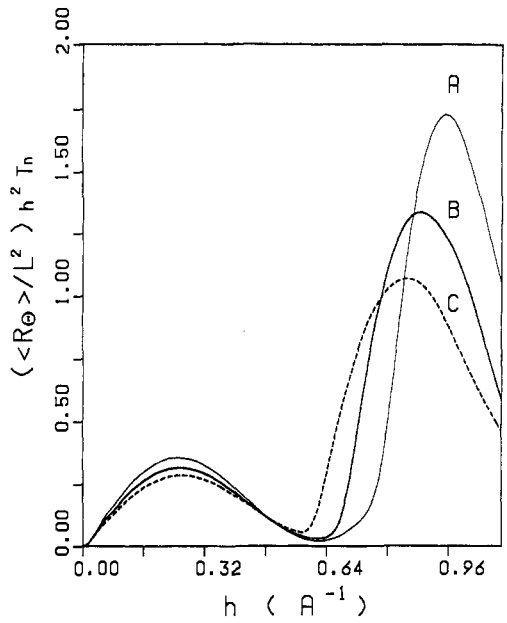

Figure 2. Comparison between rigid helix models having different helical pitch per monomer unit (P_h) in the normalized Kratky plot, $\{\langle R_\theta\rangle/L^2\}h^2T_n$ vs h: (model A) P_h = 1.33 Å; (model B) P_h = 1.53 Å; (model C) P_h = 1.73 Å. Glucose residues per turn = 6, U_l = 4.25 Å, and T_n = 60 are common to all models.

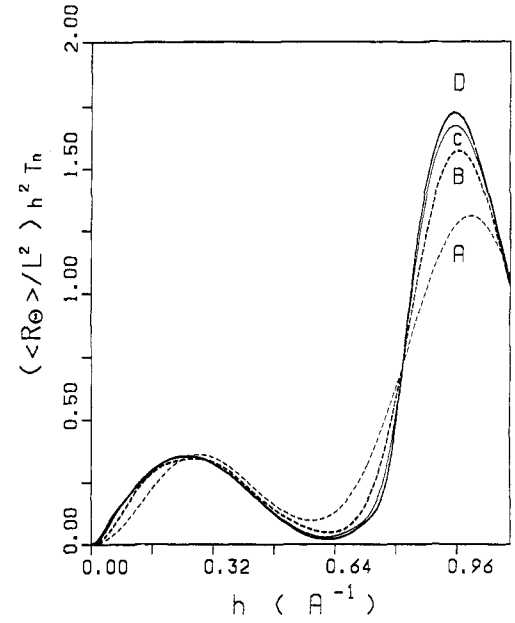

Figure 3. Effect of T_n on the normalized Kratky plot for a rigid helix model with P_h = 1.33 Å, U_l = 4.25 Å, and glucose residues per turn = 6: (model A) T_n = 12, N = 2; (model B) T_n = 24, N = 4; (model C) T_n = 42, N = 7; (model D) T_n = 60, N = 10.

polymer chain

$$f = \frac{B\{p^2 + (2N\pi R)^2\}^{1/2}}{L} \tag{50}$$

Here, it should be noted that a so-called helical fraction, g, is given by the ratio of number of monomers included in helical portions to T_n as follows:

$$g = \frac{B\{p^2 + (2N\pi R)^2\}^{1/2}/U_l}{T_n} \tag{51}$$

and so g and f are interrelated by

$$g = \left\{1 + \left(\frac{1}{f} - 1\right)\frac{U_l}{a}\right\}^{-1} \tag{52}$$

Discussion

As stated in the Introduction, a rigid helix model is one of the possible conformations of amylose in aqueous solution. If the helix has the same helical characteristics as crystalline V-amylose, it has six glucose residues per turn and P_h = 1.33 Å.[3-6] There is, however, a possibility that P_h may be slightly modified in aqueous solution. To see the effect of a variation in P_h on the scattering function, three different helices, model A with P_h = 1.33 Å, model B with P_h = 1.53 Å, and model C with P_h = 1.73 Å, are compared in Figure 2 in the form of a normalized Kratky plot, $\{\langle R_\theta\rangle/L^2\}h^2T_n$ vs h. The scattering function was computed by eq 25 for B = 1, M = 0, and T_n = 60. The magnitude of U_l, 4.25 Å, was taken from the paper of Brant et al.[34]

The scattering behaviors for the three models with different pitches do not show any significant differences in the h range lower than 0.5 Å^{-1}, and all show broad maxima near h = 0.25 Å^{-1}. However, significant differences are found in the range of h greater than 0.60 Å^{-1}. If $T_n \geq 60$, these features are independent of T_n, as seen in Figure 3. Therefore, it is concluded that a slight change in P_h may be found in the normalized Kratky plot at $h >$ 0.6 Å^{-1}. Here, it should be noted that such an effect of P_h on the scattering functions of rigid helices and also the estimated radii of gyration, 111.4, 128.1, and 144.9 Å for models A–C, respectively, are in good agreement with Brant's data[32] obtained by evaluating eq 1 on the basis of the molecular geometry of amylose (compare Figure 2 with Figure 1 in ref 32). From this fact, we consider that the present formulation of the scattering function for a rigid helix model could safely be extended to the cases of a broken helical chain and an interrupted helical chain. Although experimental data of amylose in aqueous solution are not available at present, it seems useful for further studies in this field to see the effect of the presence of freely hinged joints in a helical chain on the scattering function and to see the relation between the radius of gyration and the local conformation reflected in the scattering function.

When some flexible joints are introduced into a rigid helix having a fixing T_n, a significant effect should be observed not only on the local conformation but also on the overall conformation. In the case of T_n = 72, P_h = 1.33 Å, and glucose residues per turn = 6, the effect of B on the normalized Kratky plot is shown in Figure 4, where the values of B are assumed to be 1, 2, 4, and 6 for models A–D, respectively. The case of B = 1 corresponds to an intact helix. As is expected, it is seen that a serious effect appears not only in the range of h greater than 0.60 Å^{-1} but also in the smaller h range.

The radius of gyration of a polymer chain alone cannot provide detailed information on the local conformation of a chain. It may be obtained by studying the scattering functions of interrupted helical chains with different helical contents. In Figure 5, the radius of gyration estimated by eq 49 is plotted as a function of g for an interrupted helical chain having molecular parameters of T_n = 240, B = 4, U_l = 4.25 Å, a = 11 Å, P_h = 1.53 Å, and glucose residues per turn = 6. A minimum occurs centered near g = 0.40, and thus, we can choose a pair of models having the same $\langle R_g^2\rangle^{1/2}$. One chosen pair is model A (g = 0.125, $\langle R_g^2\rangle^{1/2}$ = 65.4 Å) and model B (g = 0.813, $\langle R_g^2\rangle^{1/2}$ = 65.4 Å) and the other is model C (g = 0.25, $\langle R_g^2\rangle^{1/2}$ = 62.7 Å) and model D (g = 0.625, $\langle R_g^2\rangle^{1/2}$ = 62.7 Å). Here, it should be pointed out that $\langle R_g^2\rangle^{1/2}$ for these models are also comparable with that for a random-coil chain, 69.6 Å. As is shown in Figure 6, despite that the radii of gyration are equal, models A and B and also models C and D can be

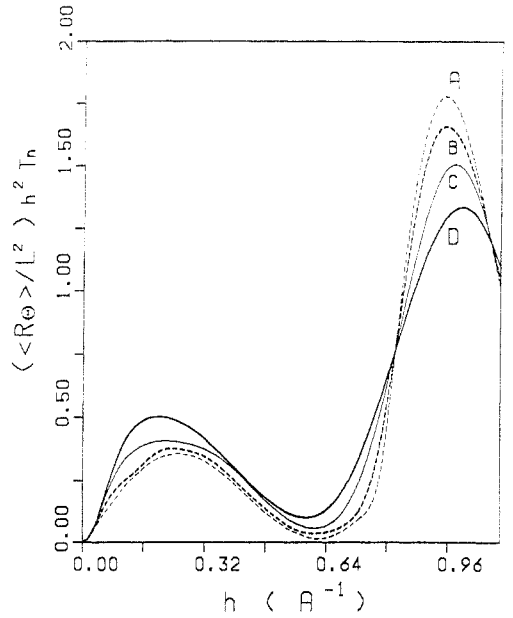

Figure 4. Effect of the number of flexible joints on the normalized Kratky plot for a broken helical chain with $T_n = 72$: (model A) $B = 1$, $N = 12$; (model B) $B = 2$, $N = 6$; (model C) $B = 4$, $N = 3$; (model D) $B = 6$, $N = 2$. $P_h = 1.33$ Å and glucose residues per turn = 6 are common to all models.

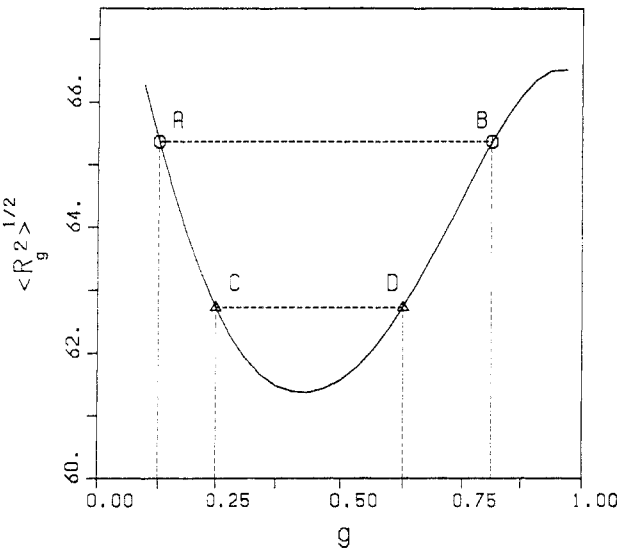

Figure 5. Radius of gyration against g for an interrupted helical chain having molecular parameters of $T_n = 240$, $B = 4$, $U_l = 4.25$ Å, $a = 11$ Å, $P_h = 1.53$ Å, and glucose residues per turn = 6. (A) and (B) in the figure correspond to model A and model B having $\langle R_g^2 \rangle^{1/2} = 65.4$ Å and $g = 0.125$ and $\langle R_g^2 \rangle^{1/2} = 65.4$ Å and $g = 0.813$, respectively. (C) and (D) correspond to model C and model D having $\langle R_g^2 \rangle^{1/2} = 62.7$ Å and $g = 0.25$ and $\langle R_g^2 \rangle^{1/2} = 62.7$ Å and $g = 0.625$, respectively.

clearly discriminated in their normalized Kratky plots due to their quite different local conformations.

A similar situation appears between an interrupted helical chain and a loose and extended helical chain containing some freely hinged joints. In Figure 7, an interrupted helical chain (model A) having $P_h = 1.33$ Å, $\langle R_g^2 \rangle^{1/2} = 95.4$ Å, and $g = 0.25$ is compared with a loose and extended helical chain (model B) having a longer P_h, 1.46 Å, almost the same $\langle R_g^2 \rangle^{1/2}$, 95.1 Å, and $g = 1.0$. $T_n = 480$, $U_l = 4.25$ Å, $a = 12$ Å, $B = 8$, and glucose residues per turn = 6 are common to two models. An extraordinary difference is observed between the behaviors in the Kratky plot of these models.

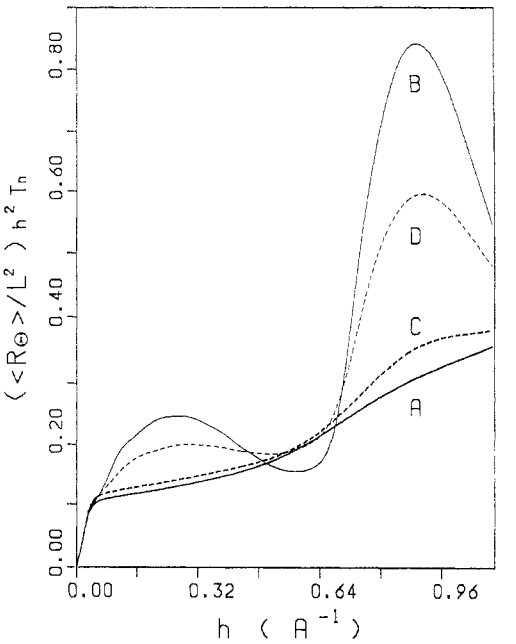

Figure 6. Comparison between the normarized Kratky plots of models A and B and between models C and D, which were characterized in Figure 5.

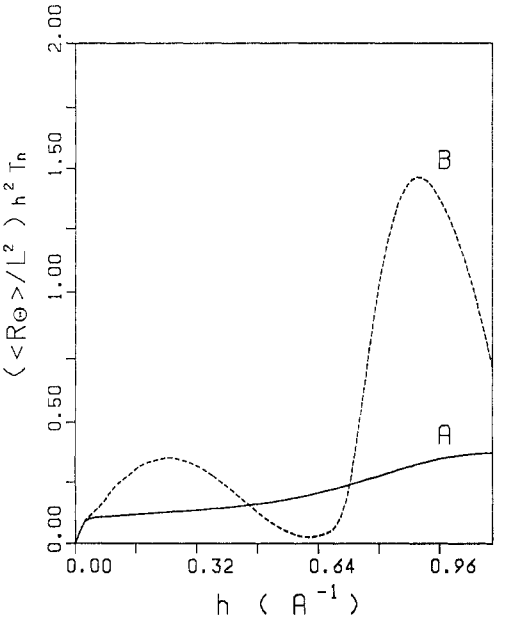

Figure 7. Comparison between the normalized Kratky plot for an interrupted helical chain (model A) having $P_h = 1.33$ Å, $\langle R_g^2 \rangle^{1/2} = 95.4$ Å, and $g = 0.25$ and a loose and extended helical chain (model B) having $P_h = 1.46$ Å, $\langle R_g^2 \rangle^{1/2} = 95.1$ Å, and $g = 1.0$. $T_n = 480$, $U_l = 4.25$ Å, $a = 12$ Å, $B = 8$, and residues per turn = 6 are common to two models.

Acknowledgment. I am indebted to Professor M. Nagasawa of Toyota Technological Institute for valuable discussions.

References and Notes

(1) Hanes, C. S. *New Phytol.* **1937**, *36*, 189.
(2) Rundle, R. E.; French, D. *J. Am. Chem. Soc.* **1943**, *65*, 1707.
(3) Rundle, R. E. *J. Am. Chem. Soc.* **1947**, *69*, 1769.
(4) Rundle, R. E.; Edwards, F. C. *J. Am. Chem. Soc.* **1943**, *65*, 2200.
(5) Samec, M.; Blinc, R.; Brenman, M. *J. Polym. Sci.* **1962**, *56*, S21.
(6) Zaslow, B. In *Starch: Chemistry and Technology*; Whistler, R. L., Paschall, E. F., Eds.; Academic Press: New York, 1965; p 279.
(7) Everett, W. W.; Foster, J. F. *J. Am. Chem. Soc.* **1959**, *81*, 3464.
(8) Banks, W.; Greenwood, C. T. *Makromol. Chem.* **1963**, *67*, 49.
(9) Banks, W.; Greenwood, C. T. *Carbohydr. Res.* **1968**, *7*, 349.

(10) Banks, W.; Greenwood, C. T. *Polymer* **1971**, *12*, 141.
(11) Banks, W.; Greenwood, C. T. *Staerke* **1971**, *23*, 300.
(12) Banks, W.; Greenwood, C. T. *Biopolymers* **1972**, *11*, 315.
(13) Banks, W.; Greenwood, C. T. *Carbohydr. Res.* **1972**, *21*, 229.
(14) Goebel, K. D.; Brant, D. A. *Macromolecules* **1970**, *3*, 634.
(15) Goebel, C. V.; Dimpfl, W. L.; Brant, D. A. *Macromolecules* **1970**, *3*, 644.
(16) Brant, D. A.; Dimpfl, W. L. *Macromolecules* **1970**, *3*, 655.
(17) Holló, J.; Szejtli, J. *Period. Polytech.* **1957**, *1*, 223.
(18) Szejtli, J. *Kem. Kozl.* **1969**, *31*, 59.
(19) Holló, J.; Szejtli, J. In *Starch and Its Derivatives*, 4th ed.; Randley, J. A., Ed.; Chapman and Hall Limited: London, 1968; p 203.
(20) Szejtli, J. *Staerke* **1971**, *23*, 295.
(21) Szejtli, J.; Augustat, S. *Staerke* **1966**, *18*, 38.
(22) Senior, M. B.; Hamori, E. *Biopolymers* **1973**, *12*, 65.
(23) Holló, J.; Szejtli, J. *Staerke* **1958**, *10*, 49.
(24) Szejtli, J.; Richter, M.; Augustat, S. *Biopolymers* **1967**, *5*, 5.
(25) Erlander, S. R.; Griffin, H. L. *Staerke* **1967**, *19*, 139.
(26) Erlander, S. R.; Purvinas, R. M. *Staerke* **1968**, *20*, 37.
(27) Pfannemüler, B.; Meyerhofer, H.; Schulz, R. C. *Biopolymers* **1971**, *10*, 243.
(28) Kuge, T.; Ono, S. *Bull. Chem. Soc. Jpn.* **1961**, *34*, 1264.
(29) Rao, V. S. R.; Foster, J. F. *Biopolymers* **1963**, *1*, 527.
(30) Banks, W.; Greenwood, C. T. *Starch and Its Components*; Edinburgh University Press: Edinburgh, 1975.
(31) Brant, D. A. In *The Biochemistry of Plants*; Preiss, J., Ed.; Academic Press: New York, 1980; Vol. 3, Chapter 11.
(32) Cesàro, A.; Brant, D. A. In *Solution Properties of Polysaccharides*; Brant, D. A., Ed.; ACS Symposium Series; American Chemical Society: Washington, DC, 1980; Chapter 34.
(33) Jordan, R. C.; Brant, D. A. *Macromolecules* **1980**, *13*, 491.
(34) Jordan, R. C.; Brant, D. A.; Cesàro, A. *Biopolymers* **1978**, *17*, 2617.
(35) Muroga, Y. To be published.
(36) Muroga, Y. *Macromolecules* **1988**, *21*, 2751.
(37) Hermans, J.; Hermans, J. J. *J. Phys. Chem.* **1958**, *62*, 1543.